A scaling and mapping theory for excess electrons in simple fluids

Jianshu Cao
Department of Chemistry, University of Pennsylvania, Philadelphia, Pennsylvania 19104-6323

B. J. Berne
Department of Chemistry, Columbia University, New York, New York 10027-6948

A simple scaling argument is proposed to understand the localization of excess electrons in simple fluids and to interpolate numerical results of path integral simulations and reference interaction site—polaron theory. A mapping is found between an impenetrable object of arbitrary geometry and a spherical hard sphere. Numerical simulations of solvated electrons in atomic and diatomic solvents are used to demonstrate the validity and applicability of these scaling and mapping schemes. © *1995 American Institute of Physics.*

I. INTRODUCTION

The behavior of excess electrons dissolved in fluids has been the subject of many theoretical studies.[1–5] In the gas phase or the dilute liquid phase, the electron assumes a quasifree particle state where scattering from the disordered media gives rise to diffusive motion. As the solvent density increases, electrons exhibit different properties depending on the nature of solvent and the electron–solvent interactions. Generally speaking, the electronic states can be properly catalogued as *extended* and *localized* states. For systems with strong electron–solvent repulsions, such as helium, density fluctuations cause the electron to be *self-trapped*. Since electron–solvent repulsion excludes the solvent molecules from the region occupied by the electron, the solvent molecules rearrange to form a cavity centered at the centroid of the electron isomorphic chain. The electron must move with the cavity and thus, the electronic mobility is very small. Therefore the *excluded volume effect* explains the mechanism of electron localization.

Coker *et al.* performed path integral Monte Carlo simulations for an excess electron solvated through a realistic pseudopotential in 6-12 Lennard-Jones fluids[3] and Sprik *et al.* studied the primitive model of an electron in a hard sphere fluid in which the electron–solvent interaction is also taken to be of the hard sphere type.[2] Chandler and coworkers developed a reference interaction site-polaron theory (RISM–polaron theory) which agrees well with the hard sphere simulations.[1,6] In an attempt to compare the results of these different calculations, Laria and Chandler assumed that some appropriately chosen hard sphere models could mimic the effects of more realistic continuous pseudopotential models. With this idea and a hard sphere radius as a single adjustable parameter, they showed that the results of different models could indeed be related. This immediately raises a question: for a general short range potential, how should one choose the effective radius of the equivalent hard sphere interaction.

Since the electron structure is predominantly determined by the excluded volume effect, the short range repulsive potential can be adequately modeled as a hard sphere potential with a single parameter d specifying the closest distance the electron can come to the center of a solvent molecule. The electron–solvent interaction at normal temperatures is dominated by low energy s-wave scattering provided the electron thermal wavelength ($\lambda = \sqrt{\hbar^2 \beta / m}$) is much smaller than the effective range of the repulsive interaction. As is well known, the phase shift for low energy s-wave scattering is characterized by a single parameter, the scattering length, and is otherwise independent of the details of the interaction potential.[7] The scattering length for the hard sphere interaction is its radius d. The hard sphere model proves ideal for describing excluded volume effects and it seems reasonable that systems with a short range repulsion can be effectively represented by this primitive model with the radius d identified as the scattering length.

In fact, similar ideas have been proposed before. In the Green function Monte Carlo study of the ground state of many-body quantum systems, Kalos, Levesque, and Verlet[8] related the simulated properties of hard sphere systems to more realistic smooth forces. They separated the interaction potential of liquid helium into a short range repulsion and a long range attraction, the latter being treated as a perturbation. The repulsive part of the potential was modeled by a hard sphere interaction in which the radius was set equal to the scattering length of the repulsive part of the smooth potential.

Since the scattering length is introduced for constant energy scattering it is only useful in the ground state energy calculations. The solvated electron is in thermal equilibrium with its environment and thus scatters successively at different energies. The thermal distribution of energies should be taken into consideration. In a previous publication on a new hard sphere propagator,[9] the quantum electron–atom distribution function

$$g(r) = \frac{\rho(r, \beta)}{\rho_{\text{free}}(r, \beta)}, \tag{1.1}$$

was defined where $\rho(r, \beta)$ is the quantum density function at temperature β for a particle at distance r away from the scattering center and $\rho_{\text{free}}(r, \beta)$ for a free particle. $g(r)$ thus defined is obviously the quantum mechanical equivalent of the Boltzmann distribution function $e^{-\beta U(r)}$. It is then natural to use $g(r)$ to define the excluded volume as

$$V_{\text{ex}} = \frac{4\pi}{3} r_{\text{ex}}^3 = \int (1 - g(r)) d\vec{r}, \qquad (1.2)$$

where r_{ex} is the exclusion radius. Obviously the equivalent hard sphere radius d is chosen so that the excluded volume of the hard sphere interaction equals that of the real potential, i.e.,

$$V_{\text{ex}}^{\text{hd}}(d) = V_{\text{ex}}, \qquad (1.3)$$

where $V_{\text{ex}}^{\text{hd}}$ denotes the excluded volume for a hard sphere. In the classical limit this relation gives the leading term in the WCA approximation.[10] As in the classical limit, Eq. (1.3) ignores solvent effects. In the low temperature limit, d reduces to the scattering length as suggested by Kalos *et al.*[8] Obviously, if two scattering centers have the same cross section, they will have the same excluded volume.

The argument is by no means limited to the mapping of a real potential to a hard sphere potential. In fact the definition of the effective hard sphere leads to a general scaling procedure. For the primitive hard sphere model the system is fully determined by the thermal wavelength of the electron λ, the electron–solvent hard sphere radius d, the solvent molecule diameter σ as seen by other solvent molecules, and the solvent density ρ. Therefore, for electrons solvated in liquids of the same kind, there should exist a universal scaling between the localization transition and some scaled number density.

In their discussion of the theory of electron conduction in disordered materials, Ioffe and Regel[11] suggested that the electron can be found in a quasifree state only when its mean free path is larger than its thermal wavelength. Mott further proposed that the electron will localize[12] when its mean free path equals the electron wavelength. Gee and Freeman[13] examined the limitations on the Ioffe–Regal and Mott criteria in the gas phase, and found both to be valid for gases like helium and hydrogen where the electron–solvent interaction is largely repulsive (hard-sphere-like), but less accurate for other solvents in which there are also attractive electron–solvent interactions. Thus this localization criterion will only be qualitatively useful when applied to most fluids.

The applicability of the Ioffe–Regel criterion to helium and hydrogen gases is apparently due to their net repulsive interaction with electrons, which can be modeled as hard sphere systems by the procedure described earlier. Then for the hard sphere interaction the cross section is proportional to the square of its radius, so that the Ioffe–Regel criterion can be expressed as $\lambda d^2 \rho_{Mott} = $ constant. In gases like He and hydrogen the same constant is found but in gases with attractive interactions a different constants will be found depending on the strength of the attractions. Nevertheless, the implication of the criterion does lead us to define the effective density as

$$\bar{\rho} = \rho d^2 \lambda, \qquad (1.4)$$

where the wavelength is given as $\lambda = \sqrt{\hbar^2 \beta / m}$. Also we denote the localization transition by the reduced correlation length

$$\bar{R} = \frac{R}{R_{\text{free}}}, \qquad (1.5)$$

where R measures the physical size of the electron isomorphic chain[14]

$$R = \left\langle \left| \vec{r} \left(\frac{\beta \hbar}{2} + \tau \right) - \vec{r}(\tau) \right|^2 \right\rangle^{1/2}, \qquad (1.6)$$

with τ being an arbitrary imaginary time. Then the universal scaling can be expressed as

$$\bar{R} = F(\bar{\rho}), \qquad (1.7)$$

where F is a universal function. This relation captures the major contributions to the electron localization, such as, the quantum interference between different solvent sites, the solvent–solvent correlations, and solvent reorganization due to the presence of the electron. It ignores, however, the details of these factors because it is mapped onto a hard sphere system. The essence of the excluded volume effect is manifested by defining the effective density as the crucial scaling parameter. Numerical calculations based on the RISM-polaron model presented in the next section clearly support this hypothesis.

The use of the effective density [Eq. (1.4)] to predict the localization density proves to be qualitative, but its applicability as a scaling parameter in Eq. (1.7) is more general and reliable. Instead of trying to predict the transition density through a Mott criterion, we instead show that realistic systems scale according to Eq. (1.7). This approach proves to be useful and effective.

Another interesting observation arises from studying excess electrons solvated in diatomic solvents. In classical mechanics, the cross section of a nonspherical hard target is equal to the geometric cross section, that is, the area of the disc that blocks the propagation of the incident particle, whereas in quantum mechanics, the low energy scattering is dominated by the s-wave which senses the isotropic (or orientationally averaged) potential energy surface. Thus the low energy limit of electron scattering from a nonspherical impenetrable object is equivalent to the scattering from a hard sphere with the same surface area. The predictions based on this mapping will be shown to agree well with diatomic calculations.

The hypothetical scaling method not only provides useful insight but also approximately predicts the transition density at which the electron localization occurs. For both RISM-polaron and PIMC calculations, the scaling and mapping method allows us to interconvert between two different systems by altering one or two parameters based on the excluded volume relation. One finds the optimal mapping if the equivalent system resembles the unknown system the most. Details are described later along with illustrative examples.

In the following two sections, we present numerical studies that demonstrate and verify the proposed scaling and mapping schemes.

II. SOLVENT OF SPHERICAL MOLECULES

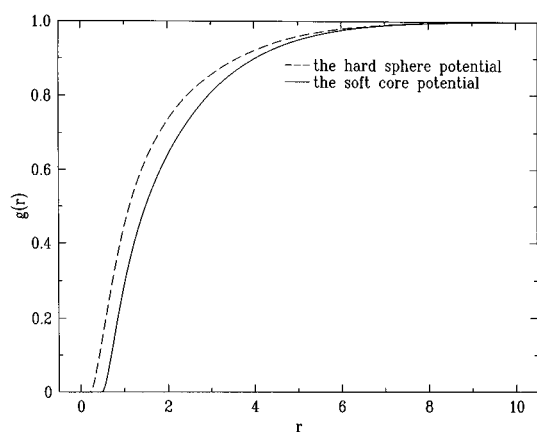The electron–solvent pseudopotential used in the simulations of Coker *et al.*[3]

FIG. 1. The quantum distribution function $g(r)$ defined by Eq. (1.1) for the electron–helium pseudopotential Eq. (2.1) at temperature 309 K and for a hard sphere potential of radius $d=0.48$ and at wavelength $\lambda=6.0$. The parameters of path integral simulations can be found in the text.

$$U(r) = \frac{A}{r^4}\left[\frac{B}{C+r^6} - 1\right], \qquad (2.1)$$

was used where A, B, and C are 0.655, 89 099, and 12 608, respectively (in the atomic units). The quantum distribution function $g(r)$ defined in Eq. (1.1) for an electron at the simulation temperature 309 K was calculated for this potential [Eq. (2.1)]. The staging Monte Carlo technique[14] was employed to generate a sequence of free particle paths. The Boltzmann factor $\exp[-\beta\Sigma_i^P U_i/P]$ was evaluated at each point on a fine grid of r and then averaged over 10^5 path integral configurations of discretization number $P=1000$. For a hard sphere potential, much faster convergence can be achieved with P less than 50 if the new hard sphere propagator[9] is used. Laria and Chandler[15] assumed for the potential given in Eq. (2.1) an equivalent primitive model of electron wavelength $\lambda=6.0\sigma$ and radius $d=0.48\sigma$ with $\sigma=2.556$ being the diameter of the solvent LJ potential. In

the rest of this paper and in the figure captions the unit of length is taken as σ, the diameter of the hard sphere solvent.

In Fig. 1 the quantum distribution functions $g(r)$ for both the potential given in Eq. (2.1) and for the equivalent hard sphere potential are plotted. The similarity of the two curves is evident although the potential surfaces themselves are very different. The calculated excluded radius r_{ex} is 2.75σ for the potential Eq. (2.1) and 2.9σ for the equivalent hard sphere. Therefore a smaller radius d would seem to be required.

To test the validity of the scaling hypothesis, we carried out RISM-polaron calculations on the primitive model with $d=\sigma/2$, σ being the solvent–solvent hard sphere diameter. Readers are referred to the papers by Chandler and co-workers for details of the RISM-polaron theory and the numerical algorithm.[1,6,15] In Fig. 2 the reduced correlation length $\bar{R}$ is plotted as functions of reduced density (defined as $\rho^* = \rho\sigma^3$) for thermal wavelength $\lambda=4\sigma$, $\lambda=6\sigma$, $\lambda=10\sigma$, and $\lambda=16\sigma$. In Fig. 3 the same set of data is plotted as functions of the effective density $\bar{\rho} = \rho d^2\lambda$. Obviously the three widely separated curves in Fig. 2 come much closer to overlapping than in Fig. 3 after the density axis is rescaled. This convergence demonstrates the adequacy of the universal scaling relation Eq. (1.7).

As observed in Fig. 2, the localization transition occurs at $\rho^*=0.3$ for $\lambda=6\sigma$ and at $\rho^*=0.15$ for $\lambda=10\sigma$. This indicates that the effective transition density is at $\bar{\rho}=0.4-0.5$. Making use of the universal relation Eq. (1.7), we can predict the transition region. In Fig. 4 the top curve stands for the upper bound and the bottom curve stands for the lower bound of the transition region. Since at small electron thermal wavelengths the number density is scaled by a parameter, the transition region will occur at high density and with a broad width. Concomitantly at large thermal wavelengths the transition will occur precipitously (with a narrow width) at a low density.

The estimation of the transition region is by no means accurate compared with systematic simulation studies. When does it hold and what factors are left out?
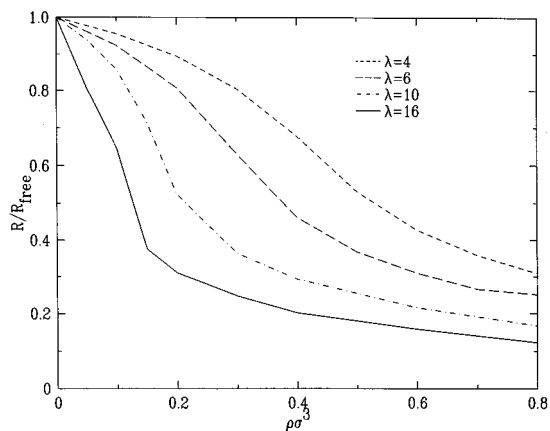

FIG. 2. The reduced correlation length $\bar{R}$ of Eq. (1.2) from RISM-polaron calculations as a function of reduced solvent density ρ^*. The results are given for the primitive model of $d=0.5$ at wavelengths 4.0, 6.0, 10.0, and 16.0.
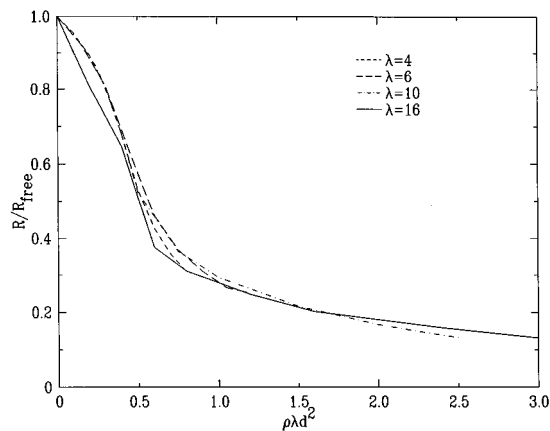

FIG. 3. The same reduced correlation function length $\bar{R}$ as a function of the effective solvent density $\bar{\rho}$. The convergence of the three curves corresponding to wavelengths 4.0, 6.0, 10.0, and 16.0 affirms the scaling hypothesis Eq. (1.7).
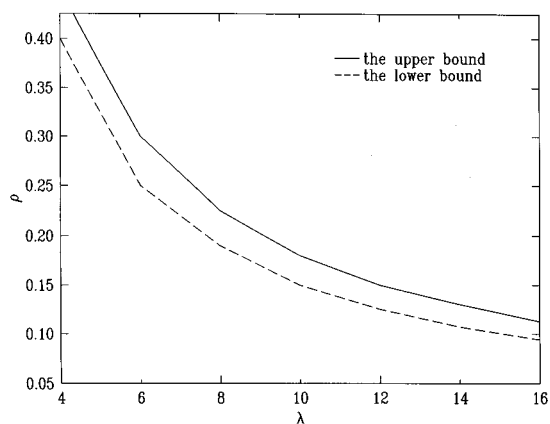
FIG. 4. The transition region of electron localization predicted by the universal scaling relation Eq. (1.7).

FIG. 5. The excluded length r_{ex} as a function of bond length L at electron wavelength $\lambda = 6\sigma$. The circles represent the results of a diatomic model with $d = 0.5$; the line is the predictions of the corresponding atomic model with $\bar{d}$ defined by Eq. (3.1).

(a) Unlike classical dynamics, the full quantum distribution in the presence of multiple solvent molecules of a particular configuration does not equal the product of quantum distribution probabilities for each molecule of the same configuration. If we compare different potentials all having the same excluded volume at the same temperature, the difference due to many body interference is minimized [see (b) below]. But if we compare systems of different electron–solvent potentials with the same excluded volume but at different temperatures, there will be nonlinear dependence on the solvent density [see (d) below]. This is responsible for the discrepancies observed in Fig. 3.

(b) Although the idealized hard sphere potential and a realistic potential such as Eq. (2.1) are very different, the quantum distribution function $g(r)$ in Fig. 1 can be very similar if the excluded volumes are approximately the same. The quantum dispersions smear out the details of local potential.

(c) The quantum distribution functions exhibit smaller curvature as the wavelength increases.[3] However, based on the universal scaling, we reason that the effective density is the primary parameter which determines the collective formation of a cavity and the electron correlation function regardless of the details of electron–solvent interaction, solvent–solvent correlation, and other factors.

(d) The simplicity of the definition of r_{ex} arises from ignoring solvent effects. Following the WCA approximation, one can devise a theory which introduces the solvent density as an additional variable in the relation Eqs. (1.2) and (1.3) such that the many-body effects of the solvent molecules can taken into account.

In practice, we can infer the reduced correlation length $\bar{R}$ of a given system from numerical data of another system according to the scaling. The method also helps to compare the RISM-polaron calculations with the realistic simulations. In addition, a realistic electron–solvent potential can be separated into a short range repulsion, which defines the equivalent hard sphere radius in Eq. (1.3), and a long range interaction, which can be incorporated directly into the RISM-polaron calculations.[16]
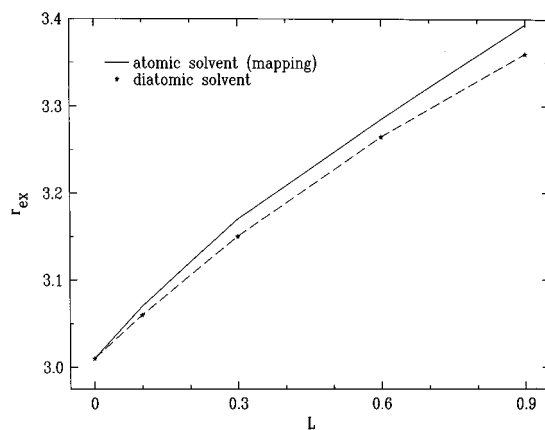
III. DIATOMIC SOLVENT

As far as low energy scattering is concerned, an impenetrable object of arbitrary geometry is equivalent to a hard sphere of the same surface area. Consider a model diatomic molecule composed of two hard spheres of radius d with their centers separated by the bond length L. The surface area is equal to that of a hard sphere of radius

$$\bar{d} = d\sqrt{1 + L/2d}. \tag{3.1}$$

Since the quantum distribution function for the diatomic molecule is not isotropic, an orientational average is introduced in the definition of $g(r)$, giving

$$g(r) = \frac{1}{4\pi} \int \frac{\rho(\vec{r}, \beta)}{\rho_{\text{free}}(r, \beta)} \, d\Omega. \tag{3.2}$$

The hard sphere propagator is modified accordingly so that the short time propagator for a particular path segment is determined only by the closer sphere. This idea can be used to simulate a hard sphere solvent for which the electron bead senses the closest hard sphere.

Path integral calculations were performed for a model diatomic fluid with $d = 0.5\sigma$, and for the corresponding hard sphere with the radius given by Eq. (3.1). The excluded length r_{ex} thus calculated is plotted in Fig. 5 as a function of bond length L for wavelength $\lambda = 6\sigma$. The results are in remarkable agreement.

Furthermore, the surface mapping is tested in the context of the scaling relation: The same excluded radius given by the mapping equation (3.1) will predict the same reduced correlation length provided the solvents are the same as well. The calculations were carried out based on the RISM-polaron theory. It turns out that only a small modification is required to formulate the atomic RISM-polaron equations for the case of polyatomic molecular solvents. Assuming that the molecule consists of n_A bonded hard-sphere sites, we can recast the RISM-polaron equation in terms of the SSOZ solution of the solvent,[17] giving
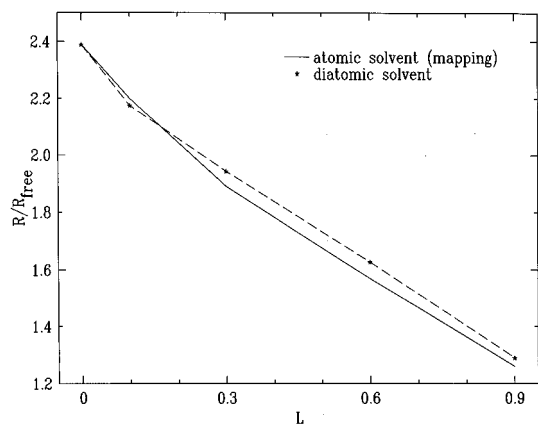
FIG. 6. The reduced correlation length $\bar{R}$ as a function of bond length L at electron wavelength $\lambda = 6\sigma$. The circles represent the results of a diatomic model with $d = 0.5$; the line is the predictions of the corresponding atomic model with $\bar{d}$ defined by Eq. (3.1).

$$I_{\text{RISM}} = \rho \sum_i \hat{C}_i(0) + \frac{1}{(2\pi)^3} \int d\vec{k} \sum_{i,j} \hat{C}_i \hat{\chi}_{ij} \hat{C}_j \hat{\omega}, \quad (3.3)$$

with the PY closure:

$$\frac{\delta I_{\text{RISM}}}{\delta C_i(r)} = 0 \quad r < d_i, \quad (3.4)$$

$$C_i(r) = 0 \quad r > d_i. \quad (3.5)$$

Here, the hats denote the corresponding spatial Fourier transformation and d_i is the hard sphere radius of the ith atom. In Eq. (3.3) $\hat{\omega}$ is the average bead-bead correlation function, C_i is the direct correlation function of atoms at the ith and electron beads, and χ is the solvent structure factor between atoms at the ith site and atoms at the jth site. The structure factor can be obtained from liquid simulations or from the SSOZ solution. In case the atomic sites on molecules are identical, Eq. (3.5) reduces to a scaler equation. In Fig. 6, the reduced correlation length $\bar{R}$ at $\rho^* = 0.4$ and $\lambda = 6.0\sigma$ is plotted as functions of bond length L for the two-site molecular solvent and for the equivalent single site atomic solvent, respectively. Again, the agreement is as expected. We speculate that this surface mapping holds in general for other geometries as long as the electron thermal wavelength is much larger than the size of the target.

IV. CONCLUDING REMARKS

In this paper we propose a universal scaling principle which reduces the study of the electron solvation problem to the determination of a single important parameter. Although the treatment is by no means comparable in accuracy to path integral simulations, it reveals the conceptual simplicity of

localization. In addition, a mapping is suggested for non-spherical molecules. Both developments provide a shortcut to the understanding of the physics of solvated electrons and serves as an auxiliary means to estimate the structure of an excess electron in cryogenic fluids.

These scaling arguments also help to elucidate why an excess electron localizes in ethane but not in methane, and localizes in n-pentane and not in neo pentane. Recently Liu and Berne[18] have shown that the introduction of repulsive sites midway along the C–C bond gives simulation results in accord with experiment. In their pseudopotential, exponential terms in the electron–solvent potential Eqs. (2.1) and (2.2) determines the hard sphere radius of the equivalent system, whereas the long range attractive tail, i.e., the electron-induced dipole interaction potential, serves as a perturbation. The major effect of the three-site ethane models is that the additional strong repulsion located at the center of the C–C bond will generate an equivalent hard sphere with larger surface area than will the two site model, a sphere with a larger d. Consequently the three site model will have a larger scaled density and will thus localize electrons at lower density than the two site model. Figure 2 of Ref. 18 gives an idea of the classical excluded regions of the electron-ethane and electron-methane pseudopotentials. And this difference accounts for the localization of electron in ethane.

[1] D. Chandler, Y. Singh, and D. M. Richardson, J. Chem. Phys. **81**, 1975 (1984).
[2] M. Sprik, M. L. Klein, and D. Chandler, J. Chem. Phys. **83**, 5689 (1987).
[3] D. F. Coker, B. J. Berne, and D. Thirumalai, J. Chem. Phys. **86**, 5689 (1987).
[4] D. F. Coker and B. J. Berne, in *Excess Electrons in Dielectric Media*, edited by C. Ferradini and J. Jay-Gerin (Chemical Rubber, Boca Raton, 1991).
[5] J. Jortner, Can. J. Chem. **55**, 1801 (1977).
[6] A. L. Nichols, III and D. Chandler, J. Chem. Phys. **84**, 398 (1986).
[7] J. J. Sakurai, *Modern Quantum Mechanics* (Addison-Wesley, New York, 1985).
[8] M. H. Kalos, D. Levesque, and L. Verlet, Phys. Rev. A **9**, 2178 (1974).
[9] J. Cao and B. J. Berne, J. Chem. Phys. **97**, 2382 (1992).
[10] J. Weeks, D. Chandler, and H. C. Andersen, J. Chem. Phys. **54**, 5237 (1971).
[11] A. F. Ioffe and A. R. Regel, Prog. Semicond. **4**, 237 (1960).
[12] N. F. Mott, Adv. Phys. **16**, 49 (1967).
[13] N. Gee and G. R. Freeman, Can. J. Chem. **64**, 1810 (1986).
[14] B. J. Berne and D. Thirumalai, Annu. Rev. Phys. Chem. **37**, 401 (1986).
[15] D. Laria and D. Chandler, J. Chem. Phys. **87**, 4088 (1987).
[16] D. Hsu and D. Chandler, J. Chem. Phys. **93**, 5075 (1990).
[17] D. Chandler, in *Studies in Statistical Mechanics*, edited by E. W. Montroll and J. L. Lebowitz (North-Holland, Amsterdam, 1981).
[18] H. Liu and B. J. Berne, J. Chem. Phys. **99**, 9054 (1993).